



Thermodynamic and Surface Properties of Ni-Si-Fe-Mo in Molten State: A Theoretical Study

Dipendra Kumar Sah^{1,2,3}, Upendra Mehta², Devendra Adhikari², Shashit Kumar Yadav^{2*}

¹Central Department of Physics, Tribhuvan University, Kirtipur, Nepal.

²Department of Physics, Mahendra Morang Adarsh Multiple Campus, Tribhuvan University, Biratnagar, Nepal.

³Department of Physics, Mechi Multiple Campus, Tribhuvan University, Bhadrapur, Nepal.

*Corresponding Author: sashit.yadav@mmamc.tu.edu.np

Submitted: October 29, 2024; Revised: May 30, 2025; Accepted: June 01, 2025

Abstract

The integral excess free energy of mixing of Ni-Si-Fe-Mo quaternary alloy was calculated at temperatures of 2700 K, 2800 K, 2900 K and 3000 K using the General Solution Model. The excess Gibbs free energy of mixing for the constituent binary subsystems was calculated in the framework of Redlich-Kister polynomial. The self-consistent thermodynamic parameters for the respective thermodynamic function were taken from the available literature data. Surface tension of the system and surface concentrations of its components were calculated in the framework of Butler's model using the determined values of partial excess free energy of each component. The activity of components increased with the rise in temperature of the system. The negative value of integral excess Gibbs free energy of mixing and surface tension of the system decreased linearly at elevated temperatures.

Keywords: Ni-Si-Fe-Mo System, Alloying Behavior, Segregating Tendency, Hetero-atomic Pairing, Surface Properties, Geometrical Model

1. Introduction

Multicomponent alloys, especially high-entropy alloys (HEAs), overtake traditional binary alloys in performance because of their high configurationally entropy and also expand the range of better-performance for resisting the

corrosion with improved damage tolerance. The numerous options for selecting alloying elements create an extensive compositional design space, enabling diverse chemical structures in multicomponent alloys[1]. They exhibit superior strength, hardness, and thermal stability, better corrosion and oxidation

resistance, enhanced fatigue performance, and radiation tolerance compared to constituent individual elements[2].

Nickel enhances corrosion resistance, toughness, ductility and formability, particularly in stainless steel and super alloys [3]. Silicon reduces the overall surface tension of the molten alloy, enabling it to spread and flow more easily, particularly in fine molds and intricate geometries [4]. Molybdenum (Mo) provides resistance to alloys like steel for chemical attack, mainly in acidic and oxidative environments due to its high surface tension [5]. As Mo has high melting point, it enhances the ability of alloys to resist deformation under prolonged exposure to high temperatures and mechanical stress. Therefore, Mo-based alloys are of considerable interest for the application in space and nuclear fields [6]. Fe-Ni-based alloys demonstrate high catalytic activity and stability for the oxygen evolution reaction (OER) and provide a low-cost alternative to traditional noble metal catalysts[7]. Therefore, the temperature and compositional dependence of the thermodynamic and surface properties of the Ni-Si-Fe-Mo alloy in liquid state have been studied in present work using a theoretical approach.

Through X-ray diffraction pattern analysis of nickel silicide, induced by Pulsed Laser Irradiation technique, Magnier et al. identified stable phases as: NiSi_2 , Ni_3Si_2 , NiSi , Ni_5Si_2 and Ni_2Si

[8]. Lavrentiev et al. studied the thermodynamic and magnetic characteristics of Fe-Ni alloys through Monte Carlo simulations, identifying the formation of intermetallic compounds such as Fe_3Ni , FeNi , and FeNi_3 [9]. Iron silicate has been found to have several distinct intermetallic phases as: Fe_3Si , Fe_5Si_3 , FeSi , $\alpha - \text{FeSi}_2$ and $\beta - \text{FeSi}_2$. Zhou et al. calculated the phase equilibria of Ni-Mo binary system through Calphad technique combined with first principles calculations and their results predicted the existence of stable intermediate Ni_2Mo , Ni_3Mo , Ni_4Mo , and Ni_8Mo phases[10]. Phase equilibria and density functional theory calculation revealed the presence of MoNi_2 and MoNi_8 metastable phases[11]. Liu et al. assessed the thermodynamic properties and phase diagram of Mo-Si binary system and reported their stable intermediate phases as Mo_3Si , Mo_5Si_3 and MoSi_2 [12]. The thermodynamic analyses and phase diagram evaluations outlined existence of stable phases of Fe-Mo system like Fe_2Mo , Fe_3Mo_2 (R-phase), the σ -phase, and the μ -phase[13].

The literature review indicates that elements like Ni, Si, Fe and Mo are highly appropriate for alloying due to their desirable properties as mentioned above. Apart from this, no specific research focusing on the thermo-physical mixing properties of the liquid Ni-Si-Fe-Mo system has been performed to date. Therefore, the system has been preferred for the study in the

work and its thermodynamic and surface properties have been studied in the temperature range 2700-3000 K using General Solution Model (GSM) and Bultler's model respectively.

2. Theory

2.1 Thermodynamic properties

The excess free energy due to mixing (ΔG_{ij}^{xs}) for binary subsystem in the molten phase can be represented mathematically using the Redlich-Kister (R-K) polynomial as[14]

$$\Delta G_{ij}^{xs} = x_i x_j \sum_{\varphi=0}^n A_{ij}^{\varphi} (x_i - x_j)^{\varphi} \quad (1)$$

where A_{ij}^{φ} are polynomial coefficients depending on temperature alone. x_i and x_j are fraction of one mole of i^{th} and j^{th} components.

The quaternary excess free energy of mixing (ΔG_M^{xs}) can be calculated in the framework of GSM using the relation[15]

$$\Delta G_M^{xs} = \Delta G_{12}^{xs} + \Delta G_{13}^{xs} + \Delta G_{14}^{xs} + \Delta G_{23}^{xs} + \Delta G_{24}^{xs} + \Delta G_{34}^{xs} + x_1 x_2 x_3 x_4 f \quad (2)$$

The term f in Equation (2) is known as the quaternary interaction coefficient and its expression can be obtained from literatures[16–18]. Expression for f involves parameters known as similarity coefficient ($\xi_{i(ij)}^k$) and deviation sum of square ($\eta(ij, ik)$) and their expressions are outlined in literature[19, 20].

The expression for the partial excess free energy associated with individual

component i (ΔG_i^{xs}) in the molten system can be given as [21]

$$\Delta G_i^{xs} = \Delta G_M^{xs} + \sum_{j=1}^m (\delta_{ij} - x_j) \frac{\partial \Delta G_M^{xs}}{\partial x_j} \quad (3)$$

The activity of component i in the alloy is computed using the relation[22]

$$a_i = x_i \exp\left(\frac{\Delta G_i^{xs}}{RT}\right) \quad (4)$$

2.2 Surface properties

For the calculation of surface properties for the liquid alloy, Butler's model can be adopted, which is expressed as[23–25]

$$\sigma = \sigma_i + \frac{RT}{s_i} \ln\left(\frac{x_i^s}{x_i^b}\right) + \frac{\Delta G_{s,i}^{xs} - \Delta G_{b,i}^{xs}}{s_i}; i=1,2,3,4 \quad (5)$$

where σ_i ($i = 1,2,3,4$) represents component's surface tension at the working temperature and x_i^s and x_i^b are the concentrations of i^{th} component in the surface and bulk molten phases respectively. Similarly, $\Delta G_{s,i}^{xs}$ and $\Delta G_{b,i}^{xs}$ stand for component's the partial excess free energy for the surface and bulk phases respectively. They are related as $\Delta G_{s,i}^{xs} = \beta \Delta G_{b,i}^{xs}$ [26], where β is the coordination number that depends on crystal structure. s_i being the surface area of a monolayer for one mole of pure element i which can be calculated by using the relation as[27]–[29]

$$s_i = f N_A^{1/3} \left(\frac{M_i}{\rho_i}\right)^{2/3} \quad (6)$$

where f (≈ 1.00) is the geometrical factor, M_i is the molecular mass, ρ_i is the density and N_A is the Avogadro's number.

3. Results and discussion

3.1 Thermodynamic properties

In thermodynamic properties, excess free energy of mixing (ΔG_M^{XS}) of the Ni-Si-Fe-Mo liquid alloy have been calculated using thermodynamic database of its constituent binary subsystems. The optimised values of self-consistent parameters for excess free energy of mixing ($\Delta G_{ij}^{XS}; i, j = \text{Ni, Si, Fe, Mo}$) of binary subsystems were taken from the available literature data and tabulated in Table 1. The values of ΔG_{ij}^{XS} have been calculated at 2000 K using Equation (1) with the aid of parameters in Table 1 and presented in Figure 1.

Table 1: R-K coefficients for ΔG_{ij}^{XS} of binary subsystems of liquid Ni-Si-Fe-Mo alloy

Systems	A_{ij}^φ [Jmol^{-1}]	Ref
Ni-Si	$A_{12}^0 = -205176.85 + 33.40446 * T, A_{12}^1 = -114240.82 + 20.34156 * T, A_{12}^2 = 116695.857 - 53.88609 * T$	[30]
Ni-Fe	$A_{13}^0 = -16911 + 5.162 * T, A_{13}^1 = -10180 + 4.147 * T$	[31]
Ni-Mo	$A_{14}^0 = -46540 + 19.53 * T, A_{14}^1 = -2915$	[32]
Si-Fe	$A_{23}^0 = -151620 + 29.39 * T, A_{23}^1 = 38960 + 2.58 * T, A_{23}^2 = 36970 - 12.76$	[33]
Si-Mo	$A_{24}^0 = -158013.3 + 12 * T$	[34]

	$T, A_{24}^1 = -20000 + 15.015 * T, A_{24}^2 = 39026.3 + 5.1567 * T, A_{24}^3 = 2461.9 - 5.5087 * T$	
Fe-Mo	$A_{34}^0 = -6973 - 0.37 * T, A_{34}^1 = -9424 + 4.502 * T$	[35]

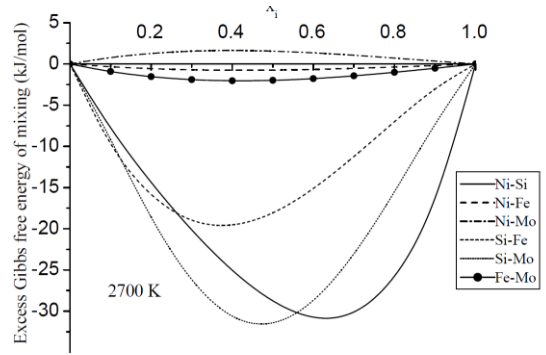


Figure 1 Compositional dependence of ΔG_{ij}^{XS} for binary subsystems of Ni-Si-Fe-Mo liquid alloy at 2700 K.

The calculated values of ΔG_{ij}^{XS} at 2700 K are found to be negative for Ni-Si, Ni-Fe, Si-Fe, Si-Mo and Fe-Mo binary subsystems, while they are positive for Ni-Mo throughout the whole range of concentration (Figure 1). The optimum negative values of ΔG_{ij}^{XS} are $-30.852 \text{ kJmol}^{-1}$ at $\text{Ni}_{63}\text{Si}_{37}$ for Ni-Si, $-0.764 \text{ kJmol}^{-1}$ at $\text{Ni}_{42}\text{Fe}_{58}$ for Ni-Fe, $-19.589 \text{ kJmol}^{-1}$ at $\text{Si}_{38}\text{Fe}_{62}$ for Si-Fe, $-31.549 \text{ kJmol}^{-1}$ at $\text{Si}_{47}\text{Mo}_{53}$ for Si-Mo and $-2.048 \text{ kJmol}^{-1}$ at $\text{Fe}_{42}\text{Mo}_{58}$ for Fe-Mo. In contrast, the positive optimal value of ΔG_{ij}^{XS} is 1.626 kJmol^{-1} at $\text{Ni}_{40}\text{Mo}_{60}$ for Ni-Mo. These findings indicate that among complex-forming alloys, the strength of ordering tendency follows the order: Si-Mo > Ni-Si > Si-

Fe > Fe-Mo > Ni-Fe while Ni-Mo shows demixing or homo-coordination tendency.

The excess free energy of mixing, ΔG_M^{xs} , of the Ni-Si-Fe-Mo liquid alloy at 2700 K are calculated employing the General Solution Model, using Equations (2) and parameters from Table 1. These values have been calculated at four different cross-sections, including 1: 2: 3, 2: 3: 1, 3: 2: 1 and 1: 1: 1 from the corners of each element. But the results for only Si and Mo corners are presented in the work as others showed the similar variation patterns, Figure 2(a,b).

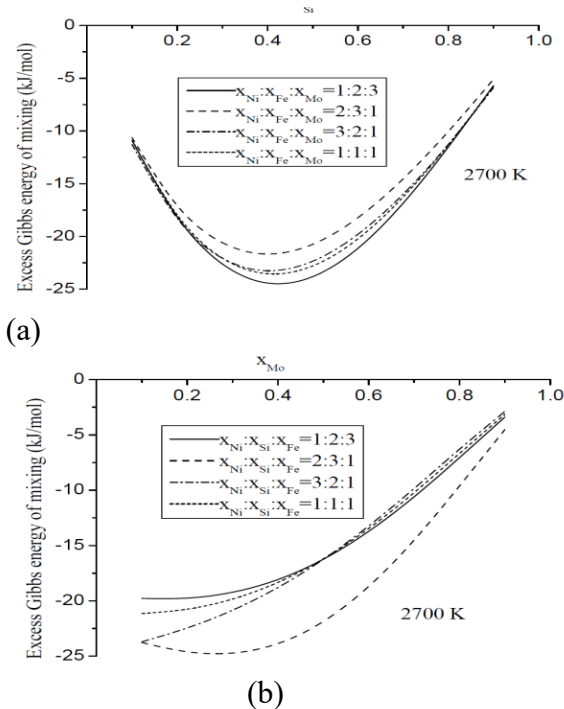


Figure 2 Compositional dependence of ΔG_M^{xs} of Ni-Si-Fe-Mo liquid alloy at 2700 K (a) from Si corner at $x_{Ni}:x_{Fe}:x_{Mo} = 1: 2: 3, 2: 3: 1, 3: 2: 1$ and 1: 1: 1 (b) from Mo corner at $x_{Ni}:x_{Si}:x_{Mo} = 1: 2: 3, 2: 3: 1, 3: 2: 1$ and 1: 1: 1.

The obtained maximum values ΔG_M^{xs} are $-21.672 \text{ kJmol}^{-1}$ at $Ni_{20}Si_{40}Fe_{30}Mo_{10}$, $-23.258 \text{ kJmol}^{-1}$ at $Ni_{30}Si_{40}Fe_{20}Mo_{10}$, $-23.560 \text{ kJmol}^{-1}$ at $Ni_{19.7}Si_{41}Fe_{19.7}Mo_{19.6}$ and $-24.487 \text{ kJmol}^{-1}$ at $Ni_{9.7}Si_{42}Fe_{19.3}Mo_{29}$ (Figure 2 (a)). The values of ΔG_M^{xs} follow the usual trends of variations at the preferred cross-sections from Si corner. ΔG_M^{xs} increases gradually with increase in concentration of Si and reaches optimum value at/around $x_{Si} = 0.4$, and decreases then after. Among these four compositions, $Ni_{9.7}Si_{42}Fe_{19.3}Mo_{29}$ has the highest strength of quaternary interaction. The occurrence of this result may be due to the largest amount of Si and Mo in $Ni_{9.7}Si_{42}Fe_{19.3}Mo_{29}$ compared to others and Mo-Si is the most interacting binary subsystem among them. However, the strengths of interaction of these quaternary complexes are less than those of Ni-Si and Si-Mo subsystems indicating that the strength of binary interaction dominates even in the quaternary melt.

Figure 2(b) shows the decrease in negative values of ΔG_M^{xs} with the increase of Mo-content at cross-sections $x_{Ni}:x_{Si}:x_{Fe} = 1: 2: 3, 3: 2: 1$ and 1: 1: 1. While it increases first upto $x_{Mo} = 0 - 0.3$ and then decreases gradually with increase in content of Mo at $x_{Ni}:x_{Si}:x_{Fe} = 2: 3: 1$. Si-content in Ni-Si-Fe-Mo at each former each cross-section is the same but is greater at $x_{Ni}:x_{Si}:x_{Fe} = 2: 3: 1$. Therefore, contribution of Si-Mo to ΔG_M^{xs} is more

in later case compared to the previous ones leading to the occurrence of the above-mentioned result. Additionally, calculated optimum ΔG_M^{XS} values of the system for $x_{Ni}:x_{Si}:x_{Fe} = 1:2:3, 2:3:1, 3:2:1$ and $1:1:1$ are -19.781kJmol^{-1} at $Ni_{15}Si_{30}Fe_{45}Mo_{10}$, -24.721kJmol^{-1} at $Ni_{23}Si_{35}Fe_{12}Mo_{30}$, -23.712kJmol^{-1} at $Ni_{45}Si_{30}Fe_{15}Mo_{10}$ and -21.146kJmol^{-1} at $Ni_{30}Si_{30}Fe_{30}Mo_{10}$ respectively. These results also show that the binary interactions among the constituents in Ni-Si and Si-Mo dominate the quaternary complex formation tendencies.

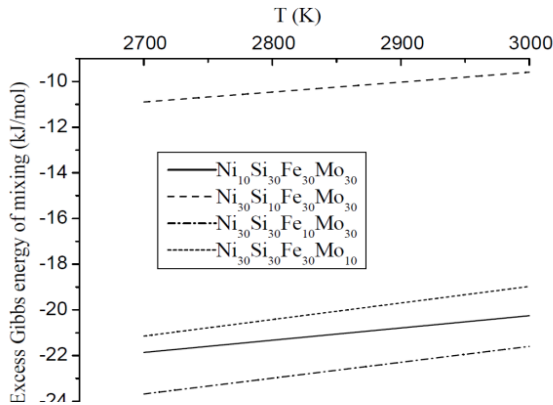


Figure 3 Temperature dependence of ΔG_M^{XS} of Ni-Si-Fe-Mo at $Ni_{10}Si_{30}Fe_{30}Mo_{30}$, $Ni_{30}Si_{10}Fe_{30}Mo_{30}$, $Ni_{30}Si_{30}Fe_{10}Mo_{30}$, and $Ni_{30}Si_{30}Fe_{30}Mo_{10}$.

of the system have been computed at compositions $Ni_{10}Si_{30}Fe_{30}Mo_{30}$, $Ni_{30}Si_{10}Fe_{30}Mo_{30}$, $Ni_{30}Si_{30}Fe_{10}Mo_{30}$, and $Ni_{30}Si_{30}Fe_{30}Mo_{10}$ and temperatures 2700, 2800, 2900 and 3000 K employing the similar methodology as mentioned above. The negative values of ΔG_M^{XS} of the system decreases linearly

with the rise in temperature, Figure 3. These results indicate the decrease in the extent of interaction among the constituents of the system to form different stoichiometric quaternary complexes, as expected.

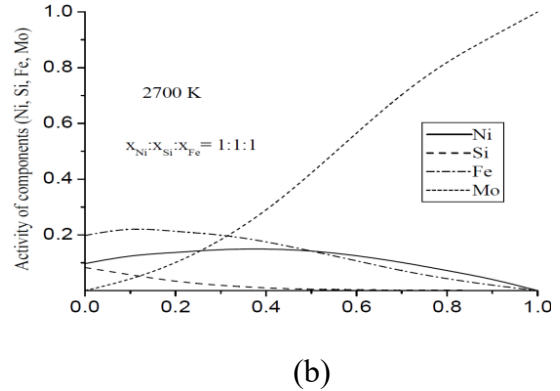
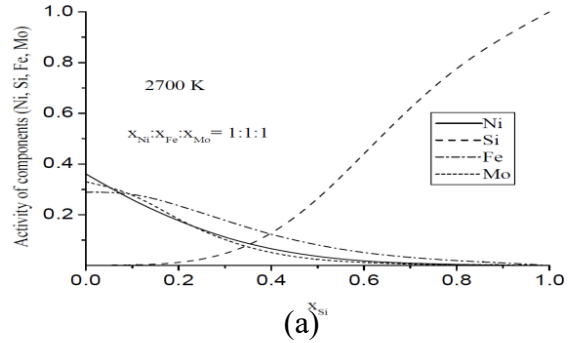


Figure 4 a_i ($i = Ni, Si, Fe, Mo$) in Ni-Si-Fe-Mo alloy at 2700 K from (a) Si corner at $x_{Ni}:x_{Fe}:x_{Mo} = 1:1:1$ and (b) Mo corner at $x_{Ni}:x_{Si}:x_{Fe} = 1:1:1$.

The values of partial excess free energy ($\Delta G_i^{XS}; i = Ni, Si, Fe, Mo$) of each element in the quaternary system have been calculated using Equations (1) and (3) with the help of parameters in Table 1. These values have been then used in Equation (4) to obtain the activity ($a_i, i = Ni, Si, Fe, Mo$) of the system's constituents. Calculations have been

done from Si corner at cross-section $x_{Ni}:x_{Fe}:x_{Mo} = 1:1:1$ and from Mo corner at $x_{Ni}:x_{Si}:x_{Fe} = 1:1:1$, Figure 4(a,b).

The values of a_i in Ni-Si-Fe-Mo for components Ni, Fe and Mo are calculated to be 0.361, 0.281 and 0.330 respectively at $x_{Si} = 0$ (Figure 4(a)). Among them, Ni shows segregating tendency with Mo and lower associating tendency with Fe compared to that between Mo and Fe as described in the case of binary subsystem. Such interactions among these components lead the occurrence of the above results. Furthermore, values of a_i for Ni, Fe and Mo decrease while that of Si increases with the fall in Si-content throughout the whole concentration range, following the usual trend. From the Figure 4(b), it is found that the values of a_{Ni} , a_{Si} and a_{Fe} are 0.097, 0.083 and 0.198 respectively when $x_{Mo} = 0$. These results occur due to the fact that complex forming tendency in Ni-Si and Fe-Si is much greater than that in Ni-Fe. Moreover, rise of Mo-content in the system causes the activities of Si and Fe to decrease in the whole concentration range, as expected. In the case of Ni, its activity increases with the increase of x_{Mo} in the range 0 – 0.4 and beyond which it decreases. The unusual trend of variation of a_{Ni} in the former ranges is due to its segregating behavior with Mo.

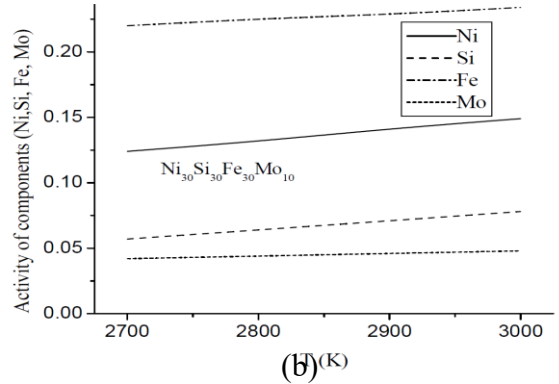
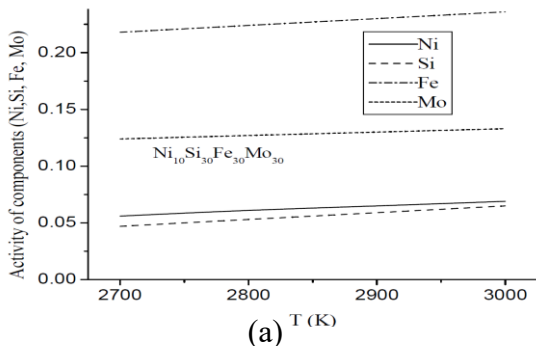


Figure 5 Temperature-dependent activity (a_i) of Ni-Si-Fe-Mo at compositions (a) $Ni_{10}Si_{30}Fe_{30}Mo_{30}$ and (b) $Ni_{30}Si_{30}Fe_{30}Mo_{10}$.

The values of a_i have also been calculated for two fixed compositions $Ni_{10}Si_{30}Fe_{30}Mo_{30}$ and $Ni_{30}Si_{30}Fe_{30}Mo_{10}$ at temperatures 2700, 2800, 2900, and 3000 K using the previously mentioned method. The results so calculated are graphically displayed in Figure 5 (a,b). It can be observed that with the increase, activities to increase in compounds $Ni_{10}Si_{30}Fe_{30}Mo_{30}$ and $Ni_{30}Si_{30}Fe_{30}Mo_{10}$ of alloy. This temperature variation of a_i is in usual trend and indicate the mixing tendency among the elements of the system, further justifying the results obtained from the analysis of ΔG_M^{xs} .

3.2 Surface properties

The surface tension (σ) of the quaternary system at 2700 K has been determined using the Butler model (Equations (5) and (6)). This calculation utilizes the previously determined values of ΔG_i^{xs} along with the necessary parameters provided from Table 2.

Table 2: Physical properties of components in Ni-Si-Fe-Mo

Density (ρ_i) [kgm^{-3}]	Ref.
$\rho_{\text{Ni}} = 7905 - 1.19(T - 1727)$	[36]
$\rho_{\text{Si}} = 2530 - 0.35(T - 1683)$	
$\rho_{\text{Fe}} = 7030 - 0.88(T - 1809)$	
$\rho_{\text{Mo}} = 9340 - 0.50(T - 2880)$	[37]
Surface tension (σ_i) [Nm^{-1}]	Ref.
$\sigma_{\text{Ni}} = 1.778 - 0.00038(T - 1727)$	[36]
$\sigma_{\text{Si}} = 0.865 - 0.00013(T - 1683)$	
$\sigma_{\text{Fe}} = 1.872 - 0.00049(T - 1809)$	
$\sigma_{\text{Mo}} = 2.25 - 0.00031(T - 2880)$	

The calculated surface tension values are plotted as a function of concentration from Si-corner at $x_{\text{Ni}}:x_{\text{Fe}}:x_{\text{Mo}} = 1:2:3, 2:3:1, 3:2:1$ and $1:1:1$ (Figure 6(a)) and from Mo-corner at $x_{\text{Ni}}:x_{\text{Si}}:x_{\text{Fe}} = 1:2:3, 2:3:1, 3:2:1$ and $1:1:1$ (Figure 6(b)).The values of the surface tension of individual components(σ_i) Ni, Si, Fe and Mo at 2700 K are calculated to be 1.40826, 0.73279, 1.43541 and 2.3058 Nm^{-1} respectively.Because of the least value of σ_{Si} , the surface tension (σ) of the quaternary alloy decreases with the rise in bulk concentration Si(x_{Si})(Figure 6 (a)). It is also seen that σ of the system at cross-section $x_{\text{Ni}}:x_{\text{Fe}}:x_{\text{Mo}} = 1:2:3$ for any fixed value of x_{Si} is found to be highest compared to other cross-sections. As the value of σ_{Mo} is the most compared to other elements in the system, the above result has been occurred.

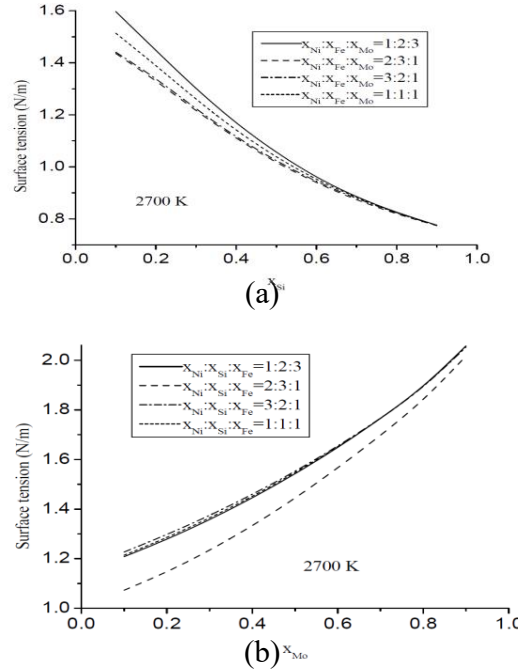


Figure 6Surface tension variation with concentration in Ni-Si-Fe-Mo at 2700 K from (a) Si-corner for $x_{\text{Ni}}:x_{\text{Fe}}:x_{\text{Mo}} = 1:2:3, 2:3:1, 3:2:1$ and $1:1:1$ (b)Mo-corner for $x_{\text{Ni}}:x_{\text{Si}}:x_{\text{Fe}} = 1:2:3, 2:3:1, 3:2:1$ and $1:1:1$.

Figure 6 (b) reveals that the value of σ increases gradually with the increase in Mo content in the system at all selected cross-sections. Additionally, it is found that the value of σ for the cross-section $x_{\text{Ni}}:x_{\text{Si}}:x_{\text{Fe}} = 2:3:1$ is the least compared to others. This result might have been occurred as Si-content is most and that of Fe is least among Ni, Si and Fe, and also their surface tension is in the order of $\sigma_{\text{Fe}} > \sigma_{\text{Ni}} > \sigma_{\text{Si}}$ at this cross-section. Furthermore, the surface tension of the system for cross-sections $x_{\text{Ni}}:x_{\text{Si}}:x_{\text{Fe}} = 1:2:3, 3:2:1$ and $1:1:1$ at any fixed value of x_{Mo} is found to be almost the same. The occurrence of this

result may be because of the fact that Si-content in the system for these three cross-sections at any fixed value of x_{Mo} is same and also as Ni and Fe have comparable value of surface tension, the interchange in their composition does not affect the surface tension value.

Moreover, σ -value the system at compositions $Ni_{70}Si_{10}Fe_{10}Mo_{10}$, $Ni_{30}Si_{10}Fe_{30}Mo_{30}$, $Ni_{30}Si_{30}Fe_{10}Mo_{30}$ and $Ni_{30}Si_{30}Fe_{30}Mo_{10}$ have been calculated for temperatures 2700, 2800, 2900 and 3000 K. The calculated values of σ are plotted as a function of temperature in Figure 7. Due to the increase of temperature, linear fall in σ -value is observed and it is in usual trend. Moreover, the rate of fall of σ -value with respect to temperature ($\frac{d\sigma}{dT}$) in the system at compositions $Ni_{70}Si_{10}Fe_{10}Mo_{10}$, $Ni_{30}Si_{10}Fe_{30}Mo_{30}$, $Ni_{30}Si_{30}Fe_{10}Mo_{30}$ and $Ni_{30}Si_{30}Fe_{30}Mo_{10}$ have been found to be -0.0004 , -0.0004 , -0.0002 and $-0.0003 \text{ Nm}^{-1}\text{K}^{-1}$ respectively.

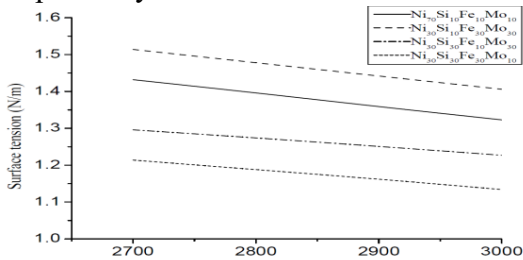


Figure 7 Temperature dependence of surface tension of Ni-Si-Fe-Mo at fixed compositions $Ni_{70}Si_{10}Fe_{10}Mo_{10}$, $Ni_{30}Si_{10}Fe_{30}Mo_{30}$, $Ni_{30}Si_{30}Fe_{10}Mo_{30}$ and $Ni_{30}Si_{30}Fe_{30}Mo_{10}$.

The calculated values of the surface concentrations of each component (x_i^s ; $i = Ni, Si, Fe, Mo$) are plotted against the concentration of Si (x_{Si}) for the cross-sections $x_{Ni}:x_{Fe}:x_{Mo} = 1:1:1$ (Figure 8 (a)) and against x_{Mo} for $x_{Ni}:x_{Si}:x_{Fe} = 1:1:1$ (Figure 8(b)). The values of x_{Ni}^s , x_{Fe}^s and x_{Mo}^s in the system at $x_{Si} = 0$ are 0.475, 0.420 and 0.097 respectively, Figure 8 (a). These results occurred as surface tension of Ni, Fe and Mo are in the order of $\sigma_{Mo} > \sigma_{Fe} > \sigma_{Ni}$. Furthermore, x_{Si}^s increases gradually with the increase in its bulk concentration where as x_{Ni}^s , x_{Fe}^s and x_{Mo}^s decrease in the entire range of x_{Si} , as expected.

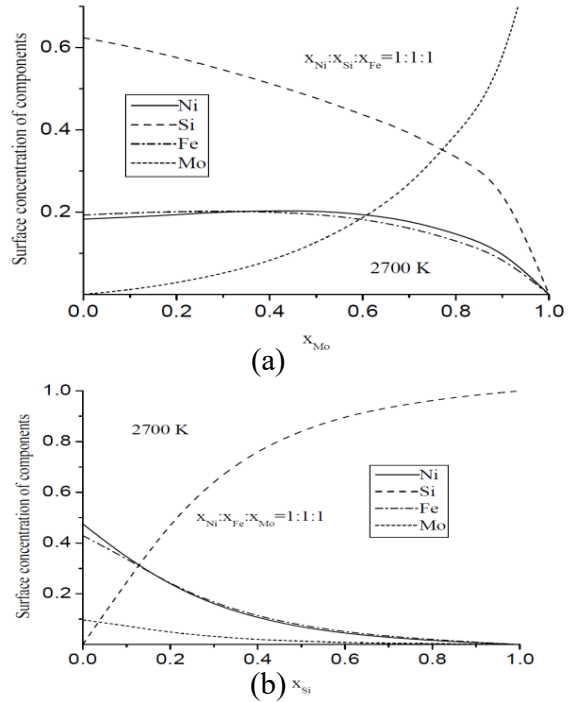


Figure 8 Compositional variations of x_{Si}^s , x_{Ni}^s , x_{Fe}^s and x_{Mo}^s in the Ni-Si-Fe-Mo liquid alloy at 2700 K from (a) Si-corner at $x_{Ni}:x_{Fe}:x_{Mo} = 1:1:1$ and (b) Mo-corner at $x_{Ni}:x_{Si}:x_{Fe} = 1:1:1$.

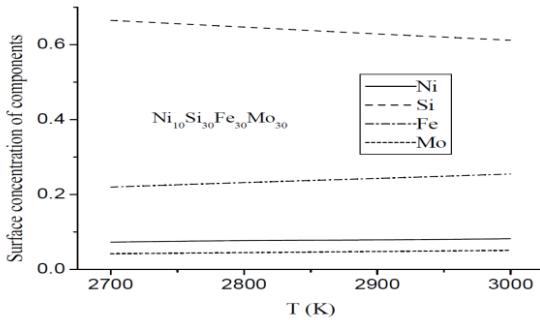


Figure 9 Temperature dependence of surface concentration for constituent components in Ni-Si-Fe-Mo melt at the fixed composition $Ni_{10}Si_{30}Fe_{30}Mo_{30}$.

From the Figure 8 (b), it is observed that surface concentrations of Ni and Fe are almost the same and do not vary so significantly in the range $x_{Mo} = 0 - 0.6$. The occurrence this result may be due to the comparable values of surface tension of Ni and Fe. Apart from this, when $x_{Mo} = 0$, components Ni, Si and Mo are observed to have surface concentrations of 0.183, 0.624 and 0.193 respectively. The value of x_{Si}^s is found to be very low compared to Ni and Fe.

The calculated values of x_i^s of components in Ni-Si-Fe-Mo melt at the composition $Ni_{10}Si_{30}Fe_{30}Mo_{30}$ are plotted against temperatures for the range 2700 -3000 K in Figure 9. The value of x_{Si}^s decreased with the rise in temperature whereas those of x_{Ni}^s , x_{Fe}^s and x_{Mo}^s increased in the entire range. The presence of much more content of Si on the surface of liquid system compared to others may cause the occurrence of above results.

4. Conclusion

From the present study, the following conclusions can be drawn:

1. The Ni-Si-Fe-Mo liquid system shows the mixing behavior in the temperature range 2700-3000 K.
2. The strength of quaternary interactions in the system decreased linearly with the increase of the temperature.
3. Activities of components in the system increased with the increase in temperature.
4. The surface tension of the system decreased with the increase of Si-content while increased with the increase of Mo content.
5. The surface tension of the system decreased linearly with the increase in temperature.
6. Concentration of Si on the surface of liquid is more than that in the bulk.
7. The surface concentration of Si decreased whereas those of Ni, Fe and Mo increased with the increase in temperature of the system.

Conflict of Interest Statement

The authors state that they have no financial or personal conflicts of interest that could have affected the findings or interpretation of this study.

References

- [1] J. Y. Zhang *et al.*, “High-entropy alloys: A critical review of aqueous corrosion behavior and mechanisms,” *High Entropy Alloy. Mater.*, vol. 2, pp. 195–259, 2023.
- [2] D. Chung, H. Kwon, C. Eze, W. Kim, and Y. Na, “Influence of Ti addition on the strengthening and toughening effect in CoCrFeNiTi_x multi principal element alloys,” *Metals (Basel)*, vol. 10, p. 1511, 2021.
- [3] H. H. Pariser, N. R. Backeberg, O. C. M. Masson, and J. C. M. Bedder, “Changing nickel and chromium stainless steel markets - A review,” *J. South. African Inst. Min. Metall.*, vol. 118, pp. 563–568, 2018.
- [4] B. Callegari, T. N. Lima, and R. S. Coelho, “The influence of alloying elements on the microstructure and properties of Al-Si-based casting alloys: A review,” *Metals (Basel)*, vol. 13, p. 1174, 2023.
- [5] S. Metals, “High-performance alloys for resistance to aqueous corrosion,” *SM Aqueous Corros. B.*, vol. 28, p. 68, 2000.
- [6] D. Lang, *Characterization of the precipitation mechanism in the molybdenum based alloy MHC*, Master’s thesis, Montanuniversität Leoben, Nov. 2012.
- [7] L. Magnier *et al.*, “Fe–Ni-based alloys as highly active and low-cost oxygen evolution reaction catalyst in alkaline media,” *Nat. Mater.*, vol. 2, pp. 252–261, 2024.
- [8] S. Tamir, S. Altshulin, and J. Zahavi, “Laser-induced nickel silicide formation,” *Thin Solid Films*, vol. 202, pp. 257–266, 1991.
- [9] M. Y. Lavrentiev, J. S. Wrobel, and S. L. Dudarev, “Magnetic and thermodynamic properties of face-centered cubic Fe-Ni alloys,” *Phys. Chem. Chem. Phys.*, vol. 16, pp. 16049–16059, 2014.
- [10] S. H. Zhou *et al.*, “First-principles calculations and thermodynamic modeling of the Ni-Mo system,” *Mater. Sci. Eng. A*, vol. 397, pp. 288–296, 2005.
- [11] K. Yaqoob, J. C. Crivello, and J. M. Joubert, “Thermodynamic modeling of the Mo–Ni system,” *Calphad*, vol. 62, pp. 215–222, 2018.
- [12] Y. Liu, G. Shao, and P. Tsakirooulos, “Thermodynamic reassessment of the Mo-Si and Al-Mo-Si systems,” *Intermetallics*, vol. 8, pp. 953–962, 2000.
- [13] A. F. Guillermet, “The Fe-Mo (Iron-Molybdenum) system,” *Bull. Alloy Phase Diagrams*, vol. 3, pp. 359–367, 1982.
- [14] O. Redlich and A. T. Kister, “Algebraic representation of thermodynamic properties and the classification of solutions,” *Ind. Eng. Chem.*, vol. 40, pp. 345–348, 1948.
- [15] K. C. Chou, W. C. Li, F. Li, and M. He, “Formalism of new ternary model expressed in terms of

- binary regular-solution type parameters,” *Calphad*, vol. 20, pp. 395–406, 1996.
- [16] R. M’chaar, A. Sabbar, M. El Moudane, and N. Ouerfelli, “A survey of surface tension, molar volume and density for Sn–Ag–Cu–Bi–Sb quinary alloys as lead-free solders,” *Philos. Mag.*, vol. 100, pp. 1415–1438, 2020.
- [17] D. K. Sah, U. Mehta, D. Adhikari, and S. K. Yadav, “Model based study of temperature dependent thermodynamic and surface properties of Al–Ti–Ni–Cr system in liquid state,” *Phys. B Condens. Matter*, vol. 695, p. 416471, 2024.
- [18] D. K. Sah, U. Mehta, R. K. Gohivar, D. Adhikari, and S. K. Yadav, “Theoretical assessment of thermodynamic and surface properties of Ag–Al–Au–Cu liquid alloy at different temperatures,” *Appl. Phys. A*, vol. 131, p. 144, 2025.
- [19] H. Arslan and A. Dogan, “An analytical investigation for thermodynamic properties of the Fe–Cr–Ni–Mg–O system,” *Russ. J. Phys. Chem. A*, vol. 89, pp. 180–189, 2015.
- [20] K. C. Chou and S. K. Wei, “A new generation solution model for predicting thermodynamic properties of a multicomponent system from binaries,” *Metall. Mater. Trans. B*, vol. 28, pp. 439–445, 1997.
- [21] H. Arslan, “Determinations of enthalpy and partial molar enthalpy in the alloys Bi–Cd–Ga–In–Zn, Bi–Cd–Ga–Zn and Au–Cu–Sn,” *Mater. Chem. Phys.*, vol. 153, pp. 384–389, 2015.
- [22] L. Gomidželović, A. Kostov, D. Živković, and V. Krstić, “Analytic approach to alloys thermodynamics: ternary Cu–Ga–Ni system,” *Mater. Res.*, vol. 19, pp. 1026–1032, 2016.
- [23] J. A. V. Butler, “348 J. A. V. Butler,” vol. 1, pp. 348–375, 1906.
- [24] G. Kaptay, “Improved derivation of the Butler equations for surface tension of solutions,” *Langmuir*, vol. 35, pp. 10987–10992, 2019.
- [25] A. Dogan and H. Arslan, “An investigation of influencing of Sb and Bi contents on surface tensions associated with Pb-free Sn–Zn–Sb–Bi quaternary and sub-quaternary solder alloys,” *Philos. Mag.*, vol. 99, pp. 1825–1848, 2019.
- [26] D. Adhikari, I. S. Jha, and B. P. Singh, “Transport and surface properties of molten Al–Mn alloy,” *Adv. Mater. Lett.*, vol. 3, pp. 226–230, 2012.
- [27] S. K. Yadav et al., “Prediction of thermodynamic and surface properties of Pb–Hg liquid alloys at different temperatures,” *Philos. Mag.*, vol. 96, pp. 1909–1925, 2016.
- [28] A. Dogan and H. Arslan, “An investigation on surface tensions of Pb-free solder materials,”

- Philos. Mag.*, vol. 96, pp. 2887–2901, 2016.
- [29] V. Sklyarchuk, Y. Plevachuk, I. Kaban, and R. Novaković, “Surface properties and wetting behaviour of liquid Ag-Sb-Sn alloys,” *J. Min. Metall. Sect. B Metall.*, vol. 48, pp. 443–448, 2012.
- [30] Y. Du and J. C. Schuster, “Experimental investigations and thermodynamic descriptions of the Ni-Si and C-Ni-Si systems,” *Metall. Mater. Trans. A*, vol. 30, pp. 2409–2418, 1999.
- [31] H. Arslan and A. Dogan, “An analytical investigation for thermodynamic properties of the Fe-Cr-Ni-Mg-O system,” *Russ. J. Phys. Chem. A*, vol. 89, pp. 180–189, 2015.
- [32] Y. Wang, C. Yu, R. Kainuma, Y. Li, X. Liu, and K. Ishida, “Experimental investigation and thermodynamic calculation of the phase equilibria in the Cu-Mo-Ni ternary system,” *Mater. Chem. Phys.*, vol. 125, pp. 37–45, 2011.
- [33] U. Mehta, I. Koirala, S. K. Yadav, R. P. Koirala, and D. Adhikari, “Prediction of thermodynamic and surface properties of ternary Ti-Si-Fe liquid alloy,” *Model. Simul. Mater. Sci. Eng.*, vol. 28, p. 065010, 2020.
- [34] C. Guo, C. Li, P. J. Masset, and Z. Du, “A thermodynamic description of the Al-Mo-Si system,” *Calphad*, vol. 36, p. 100–109, 2012.
- [35] Z. Du, C. Guo, C. Li, and W. Zhang, “Thermodynamic description of the Al-Mo and Al-Fe-Mo systems,” *J. Phase Equilibria Diffus.*, vol. 30, pp. 487–501, 2009.
- [36] W. F. Gale and T. C. Totemeier, *Smithells Metals Reference Book*, Elsevier, 2003.
- [37] X. J. Han and B. Wei, “Thermophysical properties of undercooled liquid Co-Mo alloys,” *Philos. Mag.*, vol. 83, pp. 1511–1532, 2003.